Nanoreactors for Continuous Flow Processing: Effect of Catalyst Loading and Space-Time

Andreia J. Lopes[1], Jan C. M. van Hest[2], Pedro T. Gomes[1]

[1]DEQ, Instituto Superior Técnico, Universidade de Lisboa, Av. Rovisco Pais, 1, 1049-001 Lisboa, Portugal

[2]Department of Bio-Organic Chemistry, Eindhoven University of Technology, Den Dolech 2, 5612 AZ Eindhoven, The Netherlands.

ABSTRACT: Nanoreactors are fascinating structures that sparked the attention of researchers due to their handling of chemical transformations[1]. Employing a nanosized reactor has become an emerging trend since they have the ability of accommodating compounds that will act *in situ*[2][3]. Polymeric nanoreactors (polymersomes) are relevant for catalytic processes due to their robustness, which facilitates recycling and efficient usage of catalytic species[4][5]. Polymersomes can acquire a bowl-shape (stomatocytes) under mild conditions[6] thanks to their flexible membrane allowing a more effective entrapment of catalysts inside the "stomach". Since management of resources is a guideline for scientists[7], nanoreactors can be beneficial by minimizing reaction waste[8] and cost, as opposed to traditional catalytic pathways. In light of the green chemistry concept[9], the focus was on developing novel catalytic nanoreactors to improve the efficiency of synthetic operations that can be employed for in flow synthesis of compounds, specifically in the hydrolysis of p-nitrophenyl acetate to p-nitrophenol catalyzed by the enzyme *Candida Antarctica Lipase B* (Cal B). The biocatalytic nanosystems engineered, based on polymersomes made using PEG_{44}-PS_{140} copolymers produced by ATRP, were well defined in terms of morphology and shape. Their performance in a continuous flow setup was studied in terms of activity and leaching together with the reusability and a way of optimizing the system in smaller volumes has been reported.

Key-words: *nanoreactors, stomatocytes, continuous flow, reusability, leaching, optimization*

Introduction

Polymeric stomatocytes are a distinguished type of nanoreactors due to having a bowl-shaped structure that results from a shape transformation induced in a polymersome. Their architecture provides an improved confinement of catalysts whether they be of metallic[10] or biological[6] nature. Polymersomes are spherical shaped hollow structures comprising of a hydrophobic and hydrophilic domain and are self-assembled from amphiphilic synthetic building blocks such as poly(ethylene glycol)-*b*-polystyrene (PEG-*b*-PS)[11][12][13], polystyrene-*b*-polyisocyanopeptide (PS-*b*-PIAT)[14] or poly(*N*-isopropylacrylamide)-*b*-poly(ethylene oxide) (PNIPAM-*b*-PEO)[15] or even biodegradable copolymers[16]. Thanks to their flexible membrane, polymersomes can acquire different morphologies[17] and, therefore, via a solvent addition method reported previously[6], they can be shaped into stomatocytes. These innovative nanoparticles are capturing the attention of researchers in the field of supramolecular chemistry as they can be particularly useful for biological applications[13][16][18][19] and for catalysis applications[4][5][10][20]. However, for its use in catalysis, focus on the nanoreactor's role in protecting the enzyme and its reusability is key for efficiency, and also because there are few reports on this matter. This approach could meet the demands of "green chemistry", which poses a significant challenge to many scientists trying to make remarkable developments in the field of process chemistry and catalysis.

Candida Antarctica Lipase B (Cal B) belongs to a group of biocatalysts named lipases having many applications in the laboratory and industry. Its low cost, commercial availability and simplicity of use[21] fit the requirements of this research. Our catalytic systems should have a

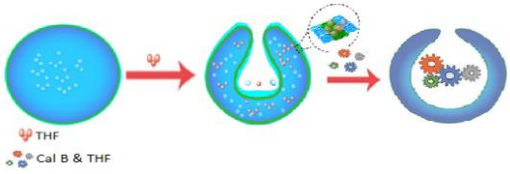

Figure 1- Supramolecular assembly of the biocatalytic nanoreactor via the solvent addition method.

compartmentalized structure enhancing their utility as a nanoreactor, allowing the positional assembly of Cal B in the nanoparticles. From a kinetic and thermodynamic point of view, compartmentalization within a nanoreactor is beneficial due to an increased stability and reaction rate[7], allowing structural and functional control over reaction pathways.

Once the stomatocytes filled with the biocatalysts were optimized in terms of morphology and size they were tested in a continuous flow reactor setup as a nanoreactor for organic synthesis. It is well acknowledged that the use of continuous flow reactors to conduct organic synthesis allows a more accurate control over reaction parameters, such as temperature and concentration, as opposed to reactions conducted in batch mode, and also facilitates the scale up of the process[22]. Besides an improved control, continuous flow technology is considered a "green" technique, since it contributes to a higher productivity and a low waste level along with the costs being low as well[23]. Herein an optimal method for the encapsulation of Cal B in the polymeric stomatocytes' cavities, and their performance in a flow system are reported. Finally, a milli-flow device was used as an attempt to optimize the process, as in recent years it has appeared to be a remarkable possibility in chemical reactor design[22][24]. In fact, it is well acknowledged that smaller devices improve production outcomes due to their extraordinary reaction control offering an effective homogeneity throughout the system, resulting in an improved mass transfer process[22][25][26].

Experimental method

The optimization of the novel polymeric nanoreactors in terms of morphology and size was a crucial step towards the success of the reaction that takes place in them. The effective internalization of the catalyst within the nanoreactors should be confirmed not to compromise its efficiency in flow. The kinetic parameters of the nanoreactors were obtained as a measure of their suitability for bigger scale processing. Therefore, the nanoreactor's performance in flow was tested in terms of activity and leaching, being the recovery and reusability of the nanoreactors in flow the main concern of this research.

Synthesis of polymersomes

The polymersomes were made using PEG_{44}-PS_{140} copolymers (20 mg), produced by Atom Transfer Radical Polymerization (ATRP), dissolved in 2 mL of THF and 3 mL of Milli-Q® were added to the solution via a syringe pump at a rate of 1 mL/h, while being stirred at 700 rpm. The final solution was collected into a dialysis membrane 12-14 kDa (Spectrum Labs) and kept under dialysis against Milli-Q® (2 L) for 24 hours, while being stirred at a rate of 560 rpm. The generated polymersome solution was collected from the membrane and stored cupped in the refrigerator at 5-8ºC.

Entrapment and quantification of Cal B

Stomatocytes formation and encapsulation of Cal B

To fold the polymersomes' membrane inward, thus forming a bowl structure (stomatocytes), 300 µL of THF was added to 500 µL of the spherical polymersomes synthesized from PEG_{44}-PS_{140} amphiphilic block copolymers, at a rate of 300 µL/h via a syringe pump, while mixing the solution at 700 rpm. After an hour, spin filtration for at least 30 minutes using 100 µm centrifugal filters at a speed of 30000 rpm was required to remove the organic solvent. The retained fraction was collected from the filters into a vial and added to 1 mL of the biocatalytic aqueous solution (3 mg/mL of Cal B). Via a syringe pump a second aliquot of THF (150 µL) was added after stirring for 30 minutes at 700 rpm to seal the stomatocytes, promoting their closure to internalize the enzymes within these polymeric structures. It should be mentioned that Cal B was suitable especially for encapsulation as its contact with organic solvent did not affect at all the enzymatic activity nor the intrinsic properties of the catalyst. Nevertheless, via a second spin filtration, it was possible to ensure the removal of any enzyme residue left on the stomatocytes' surface. Once that all the THF is filtered off and the proper amount of fresh Milli-Q® was replaced in the sample the final concentration of the sample was adjusted to the initial concentration. The final addition of Milli-Q® water was also necessary to bring the stomatocytes membrane from a flexible form (when the organic solvent was present) to a rigid form (when only water was the solvent). The biocatalytic stomatocytes were collected and stored cupped in the refrigerator at 5-8ºC.

All the samples were analyzed using Scanning Electron Microscopy (SEM), Transmission Electron Microscopy (TEM), Dynamic Light Scattering (DLS). DLS measurements were conducted to determine the size and polydispersity index (PdI) of the nanoparticles as well as SEM/TEM to verify whether the resultant morphology was adequate.

To check whether the enzyme encapsulation procedure was effective, Asymmetric Field Flow Fractionation (AF4) measurements were made to verify if there was any leakage of Cal B or if it was present on the outer surface of the stomatocytes. TEM and SDS-page also provide evidence of the enzyme's internalization.

SDS-PAGE analysis

SDS-polyacrylamide gel electrophoresis was performed using a Miniprotean tetra-cell (Bio-Rad), 4-20% running gel. To estimate the Cal B enzyme's yield (quantity) in the stomatocytes, a calibration curve was designed by running a dilution series of free enzyme and two samples of stomatocytes filled with the same enzyme in parallel, as well as Dual Color protein standard (Bio-Rad) was electrophoresed on the SDS-PAGE gel. The Dual Color protein standard (Bio-Rad) was used since its MW range is from 10 to 250 kDa and the enzyme under analysis has an expected MW of 33 kDa. The effective dilution series had a dilution factor of 2 obtaining 3 ppm, 1,5 ppm, 0,75 ppm and 2 ppm, 1 ppm, 0,5 ppm of free enzyme solution, of which 40 µL was mixed with 10 µL of 4X loading dye. As for the samples of stomatocytes filled with enzyme, 40 µL were collected and heated at 90 ºC during 3 to 5 minutes, to degrade the polymeric structure, and mixed with 10 µL of 4X loading dye. The gel was processed with the Pierce Silver Stain Kit (Thermo Fischer Scientific) for an effective staining followed by destaining to visualize the protein bands. Coomassie Blue did not prove effective for staining since this protein required a higher sensitivity. Although this method did not serve the purpose of quantifying the amount of Cal B encapsulated, it was able to confirm the effective internalization of the enzyme.

Quantification based on activity test

A spectrophotometric assay was conducted based on the test reaction selected for this research, which was the hydrolysis of p-nitrophenyl acetate to p-nitrophenol:

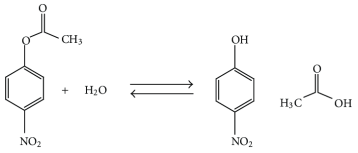

Different volumes of Cal B (2,5 mg/mL) in the required amount of phosphate buffer pH=7,5 were added to p-NPA (5 mM in DMSO, 5,0 µL) to attain the desired enzyme concentration (0, 0,5, 1,0, 1,5 and 2 mg/mL), in a total solution volume of 50 µL. A calibration curve was elaborated by monitoring the product formation during 45 minutes at 22ºC, by measuring the increase in absorbance at 405 nm, on a Tecan Spark Control V2.1 plate reader and by the formation of a bright yellow compound. Therefore, the product formation was monitored when Cal B stomatocytes and the desired buffer (4:1 v/v) were added to p-NPA (5 mM in DMSO, 5,0 µL), and the response was compared to the response of the known concentrations of Cal B allowing to determine the amount of enzyme encapsulated.

Bradford assay

Secondly, Bradford assay was performed for total protein quantitation by using the Coomassie Plus Kit (Thermo Scientific) to confirm the latter. The binding of the Coomassie blue dye to a protein in an acidic medium results in a color change from brown to blue, which changes the maximum absorption from 465 nm to 595 nm. A 2 mg/mL stock solution of Bovine serum albumin (BSA) is prepared and used as a reference. A standard curve of absorbance versus known solution concentrations, ranging from 125 to 1500 µg/mL, was made. The stomatocyte samples were previously dissolved in chloroform (4:1 v/v) to ensure that the absorbance measured was only due to the protein and not because of the polymeric membrane. For the test, 30 µL of sample is added to 1,5 mL of Coomasie Plus reagent. The equation of the BSA standard curve is used to quantify the amount of Cal B entrapped in the stomatocytes and to determine the loading efficiency.

Catalytic activity tests and kinetic parameters determination

Activity of the non-encapsulated and the encapsulated Cal B

Similarly, to the spectrophotometric assay conducted for the quantification of Cal B in stomatocytes, the product formation was monitored in the plate reader for 20 minutes at 22 ºC to compare the activity of both enzymatic forms. For the free enzyme activity measurement, Cal B (2,5 mg/mL) and phosphate buffer pH=7,5 (4:1 v/v) were added to the substrate p-NPA dissolved in DMSO (5,0 mM, 5,0 µL). As for the measurement of encapsulated Cal B activity, the initial solution was the same as for the free enzyme. The background hydrolysis was measured by the addition of the desired buffer without Cal B to the substrate (9:1 v/v). The resulting slopes of the curves were taken as a measure of the hydrolytic activity. The conversion from relative activity to specific activity (U/mg) was done using the calibration curve of the absorbance of p-nitrophenol.

Kinetic study

The kinetic parameters of both forms of Cal B were estimated to allow a comparison between free and encapsulated systems. The procedure was similar to the one previously described comparing the activity of both forms of Cal B. However, to measure the increase in absorbance at 405 nm, concentrations of substrate were used ranging from 0 to 12 mM. For the kinetic study what matters is the concentration of product formed when using different substrate concentrations. This was calculated by measuring the absorbance of the product (p-NP), which is commercially available at different concentrations and building a calibration curve.

Since the reaction can also occur without the presence of Cal B, to obtain the true increase in enzymatic reaction rate it was necessary to determine the non-enzymatic reaction rates. When Cal B was present, the enzymatic reaction rate was the sum of both enzymatic and non-enzymatic reaction rates. The true enzymatic rate is obtained by subtracting the non-enzymatic reaction rate. To determine the non-enzymatic rates, the concentration range of p-NPA used was from 0 to 12 mM and phosphate buffer pH=7,5 was added (1:9 v/v). The true enzymatic reaction rates were then plotted against the substrate concentration to produce a Michaelis-Menten model described below, for which it was possible to estimate V_{max} and K_M using a second order polynomial fitting of the enzymatic data obtained:

$$v = \frac{V_{max}[S]}{K_M + [S]}$$

where: $v =$ reaction rate; $V_{max} =$ maximum rate; [S] = substrate concentration; $K_M =$ Michaelis-Menten constant. The kinetic parameter V_{max} was used to estimate the turnover number for both forms of Cal B, since it was considered a valuable parameter for bigger scale applications. A fair comparison between the encapsulated and non-encapsulated form of Cal B in terms of their kinetic properties was reported.

Flow experiments

Continuous flow reactor system-hydrolysis of p-NPA to p-NP

The performance of stomatocytes filled with Cal B was evaluated in comparison to the performance of free enzyme (Cal B), when catalyzing the hydrolysis of p-NPA to p-NP in a continuous flow setup.

For the flow experiments, two different setups were used, which consisted of cylindrical tubes mimicking plug flow reactors. Both the systems had the same effective length of 20 cm, but different internal diameters (ID). The smaller setup had an internal diameter of 3,1 mm, while the bigger setup had an internal diameter equal to 4,1 mm.

Prior to the substrate (5 mM p-NPA dissolved in DMSO) being fed at the inlet of the reactor, via a syringe pump at a rate of 0,5 mL/h, the catalyst and phosphate buffer pH=7,5 (1:2 v/v total volume of 1,8 mL for bigger flow setup and 1,6 mL for smaller flow setup) solution were inserted at the inlet of the reactor. To test the performance of the reaction when catalyzed by the free enzyme, a 2,5 mg/mL Cal B solution was used. Eventually, the product along with the catalyst was collected at the outlet of the reactor. Furthermore, the product was separated from the catalytic stomatocytes and quantified using HPLC.

The reaction in both setups was conducted under the same conditions and in the same manner. The flow experiments were performed to study the effect of encapsulated Cal B, the effect of Cal B load in the nanoreactors and even the effect of space-time on the product outcome, as an attempt to optimize the system.

Leaching and reusability of the catalytic stomatocytes

As mentioned before, the product and catalyst were collected at the outlet of the reactor. The stomatocytes were recovered through spin filtration, using the centrifuge MSE Mistral 1000, washed with Milli-Q® and ready to be reused. The leaching was an important factor to prove that the activity loss of the encapsulated Cal B was not due to the flow configuration. To estimate the leaching, the fresh sample of stomatocytes and the sample recollected after 5 cycles of reuse were measured in terms of their specific activity via the spectrophotometric assay and of the amount of Cal B left in them via the Bradford assay.

Results and discussion

This research was aimed to demonstrate some important features relevant in industrial catalysis, which can make nanoreactors appealing tools in processes (e.g. high turnover, use in continuous setup, reusability). Moreover, this study aimed to optimize the system allowing process intensification for green processing. In the following paragraphs the main findings are discussed.

Shape and morphology characterization

Stomatocytes are prepared by inducing a shape transformation in the polymersomes, creating a cavity to facilitate the confinement of biocatalysts. Firstly, it was important to verify if

the morphology and size acquired by these nanostructures was adequate.

In terms of size, DLS measurements were made to check the dimension of these nanostructures. The nanosystems attained an average diameter between 150 and 165 nm. A slight increase in diameter was verified in the catalytic stomatocytes compared to the polymersomes, which was expected after encapsulation. The PdI is very low (<0,2) meaning that the nanoparticles did not tend to aggregate. However, further characterization techniques were used to ensure that the enzyme is effectively internalized within the stomatocytes.

Following the encapsulation procedure various techniques were used to demonstrate whether the entrapment of Cal B was successful.

Asymmetric Flow Field-Flow Fractionation (AF4) is suitable for the separation and analysis of a large distribution of particles sizes. The separation relies on the difference between the diffusion coefficients of the particles, with the smallest particles eluting first. For the analysis, aliquots of Cal B and their mixture with empty stomatocytes were injected in the AF4 separation channel. Cal B enzyme was the first to elute within the first minutes and the stomatocytes much later due to their larger size and therefore smaller diffusion coefficient (Figure 2A). Stomatocytes filled with Cal B showed only one peak corresponding to the filled stomatocytes and the peak which corresponds to the pure enzyme is not noticeable at low retention times. This indicates that the enzyme is well confined within the stomatocytes and is not adsorbed on their surface. The elution time for Cal B filled stomatocytes appears to be the same as for the empty stomatocytes, meaning that the stomatocyte's size is maintained prior to the encapsulation procedure. The shape acquired by the stomatocytes following the solvent addition method seemed adequate when observed through TEM (Figure 2B), showing completely closed stomatocytes, the strong contrast visible indicating that Cal B is well confined inside them. Although these techniques are reliable, the presence of the enzyme in the nanostructures was also confirmed by SDS-page analysis (Figure 2C).

Loading efficiency and activity of biocatalytic stomatocytes

The results of the loading efficiency obtained from the spectrophotometric assay were an overestimation when compared to the values obtained from the Bradford assay. The encapsulation efficiencies determined were not consistent (Figure 3). This variation can be due to the purification method not being the same for all the samples prepared (e.g. spin filtration time, speed, different washing volumes, use of different centrifugal units).

The results obtained from the Bradford assay were useful to calculate the specific activity (U/mg) of the stomatocytes filled with Cal B and compare them to the specific activity of the free enzyme.

The activity tests performed were helpful to determine the specific activity of Cal B in both its forms.

$$\Delta Abs = (\Delta Abs_{CalB} - \Delta Abs_{BG}) \times 60$$

$$U_{total} = \frac{\Delta Abs}{slope\ calibration\ curve}$$

$$Activity\ (U/mg) = \frac{U_{total}}{amount\ of\ Cal\ B\ (mg)}$$

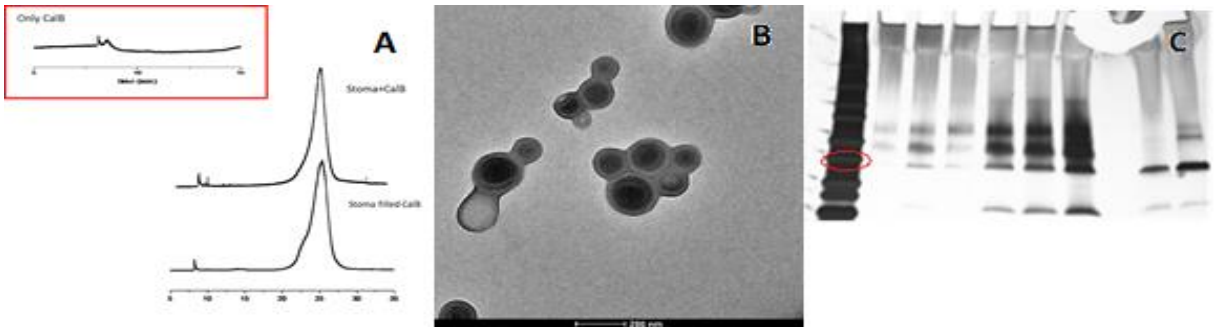

Figure 2- Characterization techniques to prove the successful encapsulation of Cal B. (A) Asymmetric flow field-flow fractionation the stomatocytes filled with Cal B and their comparative elution to the controls: empty stomatocytes and pure enzymes; (B) Transmission Electron Microscopy of the stomatocytes filled with enzyme; (C) SDS-page analysis of the stomatocytes filled with Cal B using different concentrations of Cal B as standards as means of comparison (red circle indicating the band corresponding to the enzyme's MW).

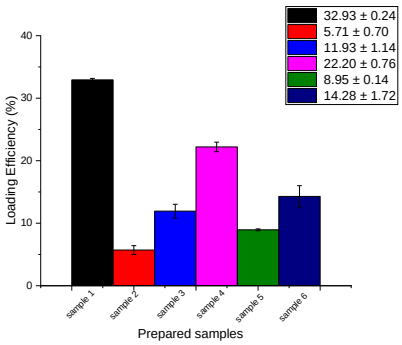

Figure 3- Loading efficiencies for different stomatocytes filled with Cal B samples.

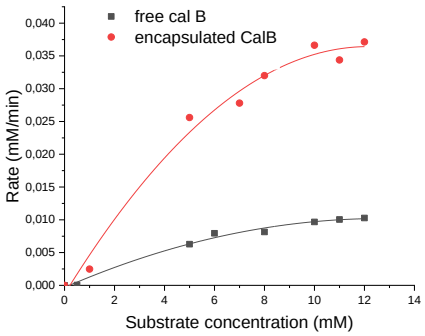

Figure 4- Polynomial Fitting of Michaelis-Menten model of enzymatic rate data for Cal B in its free form and in its encapsulated form.

The specific activity was calculated for samples with a high amount of Cal B as well as for a low amount of Cal B. The ratio of the specific activity relative to the free enzyme's activity was reported (Table 1). The specific activity of the free enzyme was 21,5 ± 2,8 U/mg. As it was mentioned before, the amount of Cal B in the stomatocytes can be a good indication of the extent of its influence on the activity.

Table 1 – Enzymatic activity after encapsulation compared with that of the free enzyme.

	Sample 1	**Sample 2**
Loading efficiency (%)	33,8	6,3
Ratio specific activity relative to free enzyme activity	8,2	1,2

We report that the enzyme was more active when entrapped. Stomatocytes which have a high loading efficiency are expected to have a higher specific activity.

Influence of entrapment conditions on enzyme kinetics

It is of particular importance to know the intrinsic kinetic properties of encapsulated Cal B in comparison to its free form offering an insight on its capability of being employed in a bigger scale process.

Saturation curves obtained by carrying out enzyme kinetic tests using encapsulated Cal B and non-entrapped Cal B (Figure 4) shows that Cal B mediated hydrolysis of p-NPA follows Michaelis-Menten model.

The maximum rate, V_{max}, is defined as the rate achieved when the enzyme molecules are saturated by substrate molecules, while the Michaelis-Menten constant, K_m, corresponds to the substrate concentration when the reaction rate is brought down to half of its maximum value. The variation observed in these parameters when the above mentioned reaction is catalyzed by either encapsulated Cal B or by free enzyme powder is displayed in Table 2.

As reported in Table 2, V_{max} value of encapsulated enzyme turned out to be higher than the value achieved for free enzyme. Since V_{max} can be considered an indication of efficiency of a reaction, this means that a reaction catalyzed by Cal B in its encapsulated form attains higher reaction rates, making the hydrolysis of p-NPA to p-NP more efficient when catalyzed by entrapped Cal B than by free Cal B. This aspect reflected on the value of k_{cat}, which was higher once again for entrapped Cal B than for the free enzyme.

Table 2 - Kinetic data for non-encapsulated and encapsulated Cal B.

	Free Cal B	**Encapsulated Cal B**
V_{max} (mM h^{-1})	0,62	2,23
k_{cat} (sec^{-1})	157,0	945,6
K_m (μM)	3790,1	3906,5

On the other hand, the K_M values, which are related to the affinity between substrate and enzyme molecules, were similar for Cal B in its encapsulated form and in its free form, suggesting that the affinity of the stomatocytes filled with Cal B towards the substrate was not so different from the free Cal B. This also proved that encapsulation of the enzyme does not affect its intrinsic proprieties.

Improvement of enzyme's performance in flow

Considering the high turnover number observed for encapsulated Cal B, activity in a continuous flow fashion was also evaluated. The performances of free Cal B and encapsulated Cal B with different loading efficiencies were tested by carrying out the same reaction in two continuous flow systems.

For the free and encapsulated enzymatic systems, it was clearly visible that the encapsulation of Cal B had a pronounced effect on the yield of product when employed in the milli-flow system (Figure 5B) as compared to the bigger flow system (Figure 5A). This result suggested that mass transfer was hindered due to the presence of a high amount of catalyst in solution when using free enzyme[27], hampering the substrate from reaching the enzyme's active sites[18][28]. The activity observed for the stomatocytes' sample also looked quite low. However, in the first test, the amount of enzyme confined in the stomatocytes was lower, so it can be concluded that overall the reaction did not suffer from significant mass transfer limitations

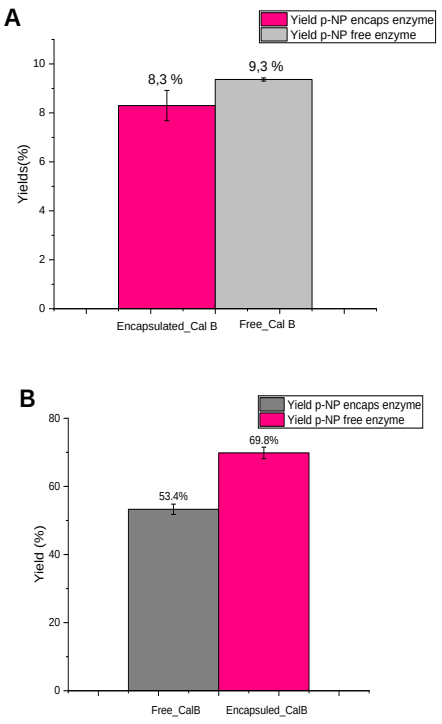

Figure 5- Yields of products attained in the two continuous flow setup using free enzyme or encapsulated enzyme. (A) Bigger flow setup (ID=4 mm); (B) Smaller flow setup (ID= 3,1 mm).

and the low yield was only due to the small amount of catalytic material employed. When the reaction was performed in the small flow-reactor, an improved yield of product was obtained for both the cases. In this case, the better performance of the nanoreactors was clearer and it can be attributed to its high surface to volume ratio, having a good dispersion in solution, thereby enhancing the diffusion of the substrate as well as improving the activity[29]. Obviously, the enhancement in the overall process was strongly dictated by the use of a smaller reactor volume, which favored the contact between catalyst and substrate.

The nanoreactors' stability was tested by performing leaching experiments in the bigger setup, employing samples with different loading efficiencies in flow. These experiments were conducted to verify whether this phenomenon was dependent on the amount of catalyst confined within the nanoreactor and to explore the extent of the nanoreactors' reusability. However, leaching was expected since these nanoreactors were non-crosslinked systems, as verified in previous works[30]. The interaction of the catalyst with DMSO used to solubilize the substrate, as well as the flow system's hydrodynamic, also contribute for the loss of catalyst confined within the nanoreactors. Figure 6 shows that a higher loaded nanoreactor (33%) experienced a great loss in activity after the first cycle of reuse, reaching a very high value that remained approximately stable for the following cycles of reuse. Meanwhile, when a lower amount of Cal B was present in the stomatocytes, it did not suffer a great loss in activity during the first cycle but tended to stabilize at a certain value during the following cycles, as the same was observed for the higher loaded nanoreactor. Besides this, in the latter case, the yield of product achieved was very low, making it impractical for any type of application. Using an intermediate loaded sample (14%) led to better results in general, its activity loss stabilizing at a more reasonable value (<50%) after the second reuse cycle. The encapsulated enzyme also retained its activity during the first cycle (~98%) suggesting that this intermediate value could be more suitable for bigger scale processes.

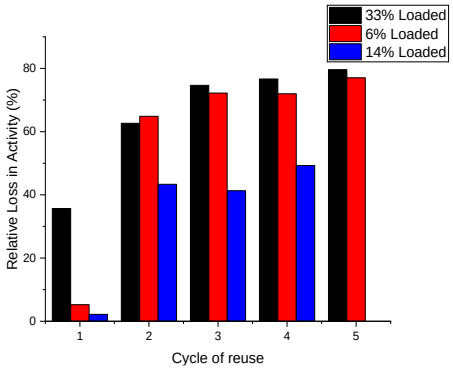

Figure 6- Losses in activity relative to the fresh sample's activity during the reusability process (5 cycles of reuse).

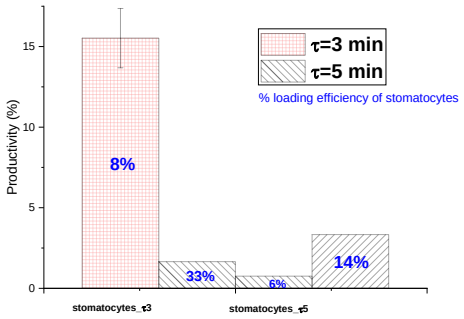

Figure 7- Productivity (%) achieved in the two setups by using stomatocytes with different load of Cal B.

In order to probe whether the activity loss was caused by enzyme deactivation or by leaching, the enzyme activity as well as the loading efficiencies were measured at the end of the 5 cycles of reuse and compared to their initial values (Table 3).

Table 3- Loading efficiency and specific activity obtained for the fresh stomatocytes and after leaching experiments for the samples tested.

		Initial	After 5 cycles
1	Loading efficiency (%)	33,8	11,1
	Specific activity (U/mg)	160,3	15,1
2	Loading efficiency (%)	6,3	2,3
	Specific activity (U/mg)	23,4	11,8

The results confirmed that the drop in activity during the cycles of reuse were due to leaching. This also can be explained by the stomatocytes with enzyme being lost during centrifugation and transfer affecting the total recovery, although this is not expected to have a big influence on the results considering the very narrow size of the filters. For the higher loaded stomatocytes, the percentage of leaching (~70%) was close to the activity loss percentage achieved in the flow experiments. The leaching was improved when a lower loaded sample of stomatocytes was employed in flow.

To investigate the influence of space time on the overall performance of the reaction catalyzed by the nanoreactors, the productivity in the two setups was calculated (Figure 7).

The productivity achieved in the smaller setup is much higher even though a lower loaded stomatocytes sample was used, which highlights that homogeneity of the reaction mixture was an essential factor to improve the overall performance of a reaction, since it promotes a better contact between the enzyme and substrate molecules, leading to a better product outcome. Similarly, to what was observed in the experiments using free enzyme, a decrease in productivity was observed when stomatocytes with higher loading efficiency are applied[31]. This effect was caused by diffusional limitations occurring throughout the system, inhibiting mass transfer; the presence of a higher amount of Cal B in the stomatocytes in the process made it more difficult for the substrate to penetrate further into the particle, hindering it from reaching the enzyme's active sites.

The various effects on the product outcome, encountered when employing the nanoreactors in flow, and seeking approaches to optimize the process, emphasized its potential for larger scale processes. Additionally, a mathematical model was generated to simulate the performance of the reaction considered.

Kinetic model

A numerical model was developed in MATLAB® to reproduce the kinetics of the reaction for the formation of p-NP using experimentally determined kinetic parameters (V_{max} and K_m).

The model is based on the practical assumption that in the spectrophotometric assay conditions, no mass transfer limitations occur. This was a reasonable assumption because of the small volume of substrate used

and the low enzymatic concentration. The developed model does not consider the amount of catalyst used, the experimental parameters previously found for that specific set of experiments. Therefore, the model can only be used to determine the amount of product formed when varying the initial concentration and when extending the reaction time (t,y output).

Some preliminary experiments were done without adding Cal B to the substrate, which showed a linear trend for the product formed versus the time, suggesting a first order dependency towards the concentration of substrate. The kinetic constant for this first order reaction was given in the script input as a guess value for all the different concentrations.

The model consists of two parts: one is the solver and one is the script containing the set of Ordinary Differential Equations (ODEs) to be solved. The model considers a set of four ODEs, two for the product formation and the other two for the substrate consumption, including the self-hydrolysis' linear rate mentioned before. The solver is comprehensive for all the constant values (such as initial concentrations and kinetic parameters) and it computes the results via an ODE45 method. Any systems of equations in the form y'=f(t,y) can be solved by all MATLAB® ODE solvers. According to this non-stiff solver, the problem had to be presented in the following way: [t,y] = ode45(odefun,t_{span},y_0) where t_{span} = [t_0, t_f], integrates the system of differential equations y'=f(t,y) from t_0 to t_f with initial conditions y_0. Each row in the solution array y corresponded to a value returned in column vector t. The final curves obtained from the model were plotted together with the experimental data to validate the model (Figure 8). Operative conditions (e.g. different amount of catalyst) need to be experimentally determined.

The results show a good agreement between the model and the experimental data obtained, when guess values for the kinetic constant of the self-hydrolysis of p-NPA (k) are given in the script. Also, it can be seen that the model had a better fitting with the experimental data for the test done using higher substrate concentrations. In fact, when the concentration of substrate was lower the value of k should decrease, but this decrease was not as linear as for the other concentrations and more difficult to predict.

Overall the model and the experimental results fit nicely, and the model can be used to predict the amount of product formed. Also, it is possible to conclude that the kinetic parameters described the system well for the operative conditions of interest. In order to consider more diverse cases, V_{max} and K_m at different operative conditions (e.g. different amount of catalyst) need to be experimentally determined.

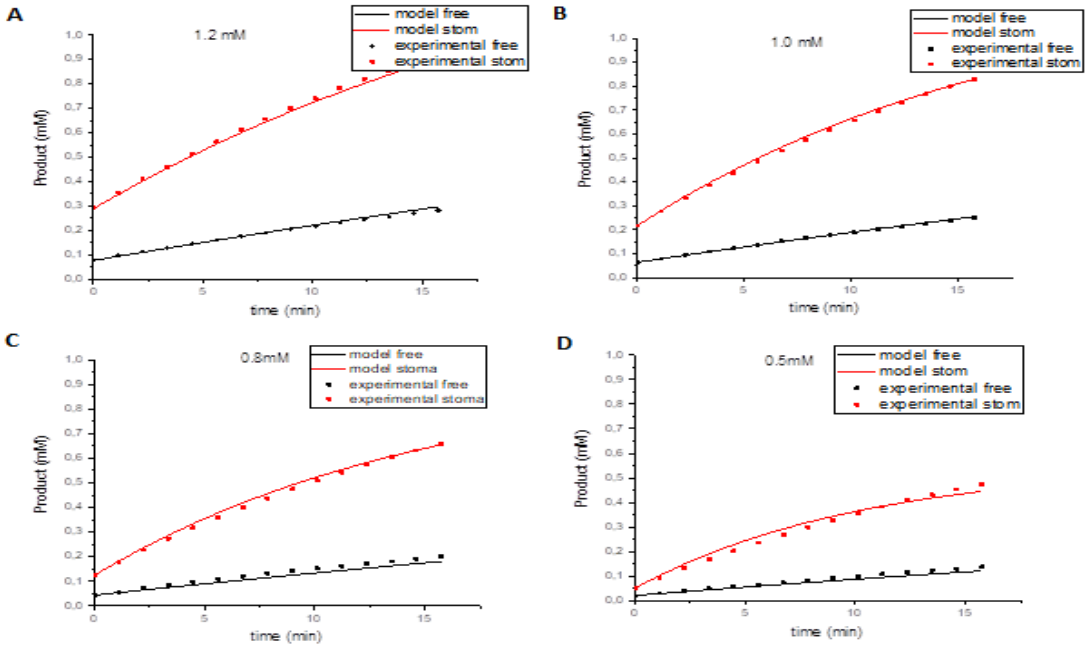

Figure 8- Experimental data (dots) collected and model predictions (lines) for the reaction rate of the p-NPA hydrolysis when the experiments where performed at different concentrations of substrate in solution (p-NPA). (A) [p-NPA]= 1,2 mM; (B) [p-NPA]= 1,0 mM; (C) [p-NPA]= 0,8 mM; (D) [p-NPA]= 0,5 mM.

Conclusions and outlook

A sustainable method to employ the Cal B nanoreactors in flow was described in this report. The encapsulated enzyme's activity was preserved in flow and its reusability was successful. While studying the effect of Cal B loaded nanoreactors in flow, it was found that using a lesser load attained a reduced leaching, but it obviously decreased the productivity. Nevertheless, the product outcome was improved by promoting a better contact between the enzyme and the substrate using a milli-flow device and decreasing the diffusional limitations.

The leaching is an aspect that can still be improved by crosslinking the membrane of the Cal B stomatocytes, therefore increasing their stability and making them more resistant.

Focusing on the encapsulated enzyme's kinetic properties, the high turnover number is an attractive feature for bigger scale processes. Moreover, its contribution in obtaining higher yields and decreasing reaction waste highlight its potential for green processing on a larger scale. By using a numerical model developed in MATLAB®, it was possible to reproduce the kinetic data collected, and the results fitted the tests which used higher concentration of substrate to a greater degree.

The encapsulation of other enzymes relevant for industrial applications following the method presented could also be useful for process intensification.

References

[1] H. Che, J. C. M. van Hest, *J. Mater. Chem. B* **2016**, *4*, 4632.

[2] J. Gaitzsch, X. Huang, B. Voit, *Chem. Rev.* **2016**, *116*, 1053.

[3] D. M. Vriezema, P. M. L. Garcia, N. Sancho Oltra, N. S. Hatzakis, S. M. Kuiper, R. J. M. Nolte, A. E. Rowan, J. C. M. Van Hest, *Angew. Chemie - Int. Ed.* **2007**, *46*, 7378.

[4] R. J. R. W. Peters, M. Marguet, S. Marais, M. W. Fraaije, J. C. M. Van Hest, S. Lecommandoux, *Angew. Chemie - Int. Ed.* **2014**, *53*, 146.

[5] M. C. M. van Oers, F. P. J. T. Rutjes, J. C. M. Van Hest, *Curr. Opin. Biotechnol.* **2014**, *28*, 10.

[6] L. K. E. A. Abdelmohsen, M. Nijemeisland, G. M. Pawar, G. J. A. Janssen, R. J. M. Nolte, J. C. M. Van Hest, D. A. Wilson, *ACS Nano* **2016**, *10*, 2652.

[7] M. T. De Martino, L. K. E. A. Abdelmohsen, F. P. J. T. Rutjes, J. C. M. Van Hest, *Beilstein J. Org. Chem.* **2018**, *14*, 716.

[8] K. C. Nicolaou, D. J. Edmonds, P. G. Bulger, *Angew. Chemie - Int. Ed.* **2006**, *45*, 7134.

[9] P. Tufvesson, W. Fu, J. S. Jensen, J. M. Woodley, *Food Bioprod. Process.* **2010**, *88*, 3.

[10] D. A. Wilson, R. J. M. Nolte, J. C. M. Van Hest, *J. Am. Chem. Soc.* **2012**, *134*, 9894.

[11] R. S. M. Rikken, H. Engelkamp, R. J. M. Nolte, J. C. Maan, J. C. M. Van Hest, D. A. Wilson, P. C. M. Christianen, *Nat. Commun.* **2016**, *7*, 1.

[12] Y. Men, F. Peng, Y. Tu, J. C. M. Van Hest, D. A. Wilson, *Polym. Chem.* **2016**, *7*, 3977.

[13] B. Iyisan, **2016**.

[14] S. M. Kuiper, M. Nallani, D. M. Vriezema, J. J. L. M. Cornelissen, J. C. M. Van Hest, R. J. M. Nolte, A. E. Rowan, *Org. Biomol. Chem.* **2008**, *6*, 4315.

[15] P. Pramanik, S. Ghosh, *J. Polym. Sci. Part A Polym. Chem.* **2015**, *53*, 2444.

[16] I. A. B. Pijpers, L. K. E. A. Abdelmohsen, D. S. Williams, J. C. M. Van Hest, *ACS Macro Lett.* **2017**, *6*, 1217.

[17] K. T. Kim, J. Zhu, S. A. Meeuwissen, J. J. L. M. Cornelissen, D. J. Pochan, R. J. M. Nolte, J. C. M. Van Hest, *J. Am. Chem. Soc.* **2010**, *132*, 12522.

[18] C. G. Palivan, R. Goers, A. Najer, X. Zhang, A. Car, W. Meier, *Chem. Soc. Rev.* **2016**, *45*, 377.

[19] P. Tanner, P. Baumann, R. Enea, O. Onaca, C. Palivan, W. Meier, *Acc. Chem. Res.* **2011**, *44*, 1039.

[20] M. C. M. van Oers, W. S. Veldmate, J. C. M. van Hest, F. P. J. T. Rutjes, *Polym. Chem.* **2015**, *6*, 5358.

[21] N. Handayani, N. Miletic, K. Loos, S. Achmad, D. Wahyuningrum, *Sains Malaysiana* **2011**, *40*, 965.

[22] P. Watts, C. Wiles, *J. Chem. Res.* **2012**, *36*, 181.

[23] C. Wiles, P. Watts, *Green Chem.* **2012**, *14*, 38.

[24] C. Reactors, **n.d.**, 1.

[25] D. T. McQuade, P. H. Seeberger, *J. Org. Chem.* **2013**, *78*, 6384.

[26] I. Denčić, S. De Vaan, T. Noël, J. Meuldijk, M. De Croon, V. Hessel, *Ind. Eng. Chem. Res.* **2013**, *52*, 10951.

[27] D. Rotticci, T. Norin, K. Hult, *Org. Lett.* **2000**, *2*, 1373.

[28] V. A. Online, C. Forsyth, S. V Patwardhan, **2013**, 1164.

[29] L. Schoonen, J. C. M. Van Hest, *Adv. Mater.* **2016**, *28*, 1109.

[30] H. P. M. De Hoog, I. W. C. E. Arends, A. E. Rowan, J. J. L. M. Cornelissen, R. J. M. Nolte, *Nanoscale* **2010**, *2*, 709.

[31] P. Adlercreutz, *Chem. Soc. Rev.* **2013**, *42*, 6406.